Analytica Chimica Acta xxx (xxxx) xxx

Contents lists available at ScienceDirect

Analytica Chimica Acta

journal homepage: www.elsevier.com/locate/aca

A highly sensitive sensor based on ordered mesoporous $ZnFe_2O_4$ for electrochemical detection of dopamine

Yarong Huang [a, b], Ying Tang [c], Shichong Xu [a], Ming Feng [a], Yongsheng Yu [a, b, *], Weiwei Yang [b, **], Haibo Li [a]

[a] Key Laboratory of Functional Materials Physics and Chemistry of the Ministry of Education, Jilin Normal University, Changchun, 130103, China
[b] MIIT Key Laboratory of Critical Materials Technology for New Energy Conversion and Storage, School of Chemistry and Chemical Engineering, Harbin Institute of Technology, Harbin, Heilongjiang, 150001, China
[c] Department of Neurology, The First Affiliated Hospital of Harbin Medical University, Harbin, Heilongjiang, 150001, China

HIGHLIGHTS

- Mesoporous $ZnFe_2O_4$ prepared successfully via a facial nanocasting method.
- Mesoporous Fe_3O_4 showed excellent detection of DA with a quick response time of 5 s, high sensitivity of 0.094 nA nM^{-1} and a lower detection limit of 0.4 nM (S/N = 3).
- Practical application of the sensor was demonstrated in PC12 cells.
- Mesoporous materials possess large specific surface area, which facilitate the mass transport and electron transfer for detection.

GRAPHICAL ABSTRACT

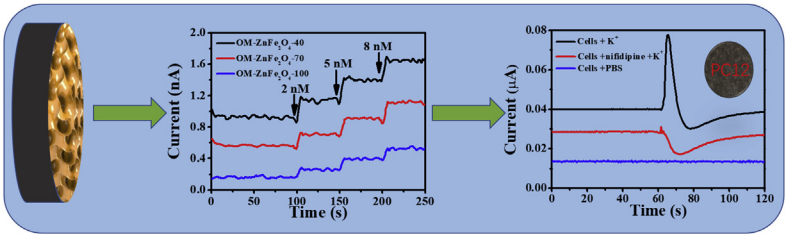

ARTICLE INFO

Article history:
Received 5 September 2019
Received in revised form
7 October 2019
Accepted 21 October 2019
Available online xxx

Keywords:
$ZnFe_2O_4$
Dopamine
Electrochemical detection
Biosensor

ABSTRACT

Accurate and sensitive detection of dopamine (DA) is fundamental to monitor and diagnose certain neurological diseases. Herein, highly ordered mesoporous $ZnFe_2O_4$ (OM-$ZnFe_2O_4$) is prepared *via* a facile nanocasting method and shows the highly sensitive in the electrochemical detection of DA. The optimized OM-$ZnFe_2O_4$-40 shows the most excellent activity for DA oxidation in a wide linear range from 2 to 600 nM with a quick response time of 5 s, high sensitivity of 0.094 nA nM^{-1} and a lower detection limit of 0.4 nM (S/N = 3). The electrode modified with OM-$ZnFe_2O_4$ is further successfully used to monitor the increase of DA concentration induced by K^+-stimulation of living PC12 cells in a neurological environment. This work offers a simple and powerful strategy for designing electrodes for detecting DA in biological systems.

1. Introduction

Dopamine (DA), as one of the neurotransmitters of inotropic synapse, has played an important role in the function of central nervous system [1]. In addition, it has critical impacts on several vital movements, such as physiological functions and cardiovascular systems, which is due to neurology disorders caused by the decrease of DA [2]. Therefore, it is essential to maintain DA in a

* Corresponding author. Key Laboratory of Functional Materials Physics and Chemistry of the Ministry of Education, Jilin Normal University, Changchun, 130103, China.
** Corresponding author.
E-mail addresses: yongshengyu@jlnu.edu.cn (Y. Yu), yangww@hit.edu.cn (W. Yang).

https://doi.org/10.1016/j.aca.2019.10.048
0003-2670/

normal level for intracellular signaling transduction and normal cell functions. Various efficient instrumental methods have been developed to realize considerable sensitive detection for DA [3–5]. Compared with fluorescence spectrometry [6] and colorimetric assay [7], electrochemical method has been considered to be one of the most excellent detection methods due to its inherent advantages, including detection simplicity, high stability and cost effectiveness [8–11]. However, conventional electrochemical method is not sufficient to sensitively detect DA at nanomolar (nM) levels.

Recent results show that the electrodes modified by catalytically active nanomaterials can increase the active specific surface area, improve effective mass transport, and achieve better control over a local microenvironment, thus proposing a variety of modified electrodes to attempt simultaneous determination of DA [12–14]. $ZnFe_2O_4$ stands out from lots of classical metal or metal oxide nanomaterials applied for biosensors due to the advantages of the good catalytic activity, stability, easy separation and excellent biocompatibility. $ZnFe_2O_4$ nanoparticles have been developed for the determination of 5-fluorouracile in drug samples with high sensitivity, good detection limits and excellent reproducibility [15]. It is reported that $ZnFe_2O_4$ nanoparticles modified carbon paste electrode can simultaneously analyze acetaminophen, epinephrine and melatonin in aqueous solution [16]. Zhao et al. [17] stated that $ZnFe_2O_4$ nanobelts prepared by coelectrospinning exhibited excellent performance with high sensitivity and fast response in the glucose detection. Compared with other nanomaterials, ordered mesoporous nanomaterials have large specific surface area, interconnected pores, and regular texture, thus providing numerous of active sites which facilitate the mass transport and electron transfer for electrochemical detection [18–22]. In this regard, it is highly desirable to prepare $ZnFe_2O_4$ with a highly ordered mesoporous structure to enhance the efficient mass and charge transfer, but still remains a great challenge.

In this work, highly ordered mesoporous $ZnFe_2O_4$ with hierarchical pore sizes and enlarged surface area was prepared by a facile nanocasting method. The optimized $ZnFe_2O_4$ shows the excellent activity for DA oxidation in the concentration ranges of 2–600 nM with a quick response time of 5 s, high sensitivity of 0.094 nA nM^{-1} and a lower detection limit of 0.4 nM (S/N = 3). The electrode modified by OM-$ZnFe_2O_4$ is used successfully to monitor the DA concentration increase induced by K^+-stimulation of living PC12 cells in a neurological environment. The results suggest that OM-$ZnFe_2O_4$ can be considered as a new type of high-efficiency biosensor for selective, sensitive and rapid determine of DA.

2. Experimental section

2.1. Synthesis of OM-$ZnFe_2O_4$

The synthesis of ordered mesoporous SiO_2 hard template (KIT-6) has been reported [23], as also described in Supporting information. 1 g of KIT-6 was impregnated in a ~0.8 M precursor solution with vigorous stirring to make sure that the template and precursor solution can be well mixed. After the solvent completely evaporated, the vessel was placed on a hitting plate at 50 °C overnight. The dried powder was transferred into a crucible and sintered at 500 °C in the air for 5 h. Then, 50 mL of 2 M NaOH solution was used to leach the SiO_2 template for 24 h. The product was collected by centrifugation and washed with distilled water for several times. Finally, the OM-$ZnFe_2O_4$ was obtained by dried the products at 60 °C. KIT-6 aged at different temperature were denoted as KIT-40, KIT-70 and KIT-100, respectively, and OM-$ZnFe_2O_4$-40, OM-$ZnFe_2O_4$-70 and OM-$ZnFe_2O_4$-100 were fabricated from KIT-40, KIT-70 and KIT-100.

2.2. Characterization

Transmission electron microscopy (TEM) was conducted on a JEOL JEM-1400. High resolution transmission electron microscopy (HRTEM) images were obtained using a Talos F200X instrument. The X-ray diffraction (XRD) patterns were recorded using a PAN-analytical X'Pert powder with Cu *Kα* radiation (λ = 1.5418 Å). The specific surface areas and pore diameter distributions of the catalysts were calculated at 77 K in N_2 on a Beishide 3H–2000 PS1 Gas Sorption and Porosimetry system by Brunauner-Emmet-Teller (BET) and Barrett-Joyner-Halenda (BJH) methods. X-ray photoelectron spectroscopic (XPS) measurements were conducted on a Perkin-Elmer PHI 5000C ESCA using twin anode Mg Ka (1253.6 eV) radiation.

2.3. Electrode construction and electrochemical measurements

The 2 mg mL^{-1} as-prepared materials mixed with 2 mg mL^{-1} Ketjen carbon were sonicated for 30 min. The mixture was then centrifuged and washed by ethanol for three times. The products were dried under N_2 and redispersed in a mixture of deionized water, isopropanol and 5% Nafion (v/v/v = 4/1/0.020) to obtain a concentration of 0.4 mg mL^{-1}. After sonication for 1 h, 10 μL of dispersion was drop casted onto a clean glassy carbon electrode (0.3 mm GCE) and dried under ambient conditions. Electrochemical experiments were conducted on a CHI660C workstation (Shanghai Chenhua, Shanghai) in a three-electrode system. Modified GCE, Ag/AgCl (in saturated KCl), and a platinum (Pt) wire were used as the working, reference, and counter electrodes, respectively. The electrodes were activated in 0.1 M phosphate buffer solution (PBS, pH 7.0) by cyclic voltammetry (CV) scanning between 0 mV and 500 mV (*vs*. Ag/AgCl) until a stable signal was obtained. CV was performed in 0.1 mM DA (PBS, pH 7.0) at a scan rate of 100 mV s^{-1}. Differential Pulse Voltammetry (DPV) was performed at various concentrations of the DA solution (PBS, pH 7.0) with a pulse width of 10 ms and an amplitude of 50 mV. An amperometric current (i)-time (t) curve was obtained at an applied potential of 0.23 V in the stirred PBS (pH 7.0) solution. The process of preparing OM-$ZnFe_2O_4$ modified electrode for DA determination was illustrated in Scheme 1.

2.4. Measuring the flux of DA released from PC12 cells

The cells were washed with phosphate buffer saline (PBS, PH = 7.0) and then dispersed in 2 mL of PBS. Amperometric-time curves of the OM-$ZnFe_2O_4$-40 electrodes were recorded in the above cell dispersion solution at a working potential of 0.23 V *vs.* Ag/AgCl. Once the background reached a stable level, 105 μL of 2.0 M KCl solution was added to the above cell dispersion. With the stimulation of KCl, PC12 cells exhibited a significant increase in current and then decrease to the background in a short time. For the inhibitory test, cells were pretreated with 50 μM of nifedipine solution for 30 min prior to KCl stimulation. These cells were stimulated with the same concentrations of KCl as normal cells, while the KCl causes relatively minor changes in current. The control experiment without cells was also carried out. Upon the addition of KCl in the detection solution, no signal was observed.

3. Results and discussion

3.1. Characterization of materials

We first prepared three kind of KIT-6 with different hydrothermal synthesis temperature (40, 70 and 100 °C), and then characterized their morphology utilizing TEM images (Fig. S1). It is

Please cite this article as: Y. Huang et al., A highly sensitive sensor based on ordered mesoporous $ZnFe_2O_4$ for electrochemical detection of dopamine, Analytica Chimica Acta, https://doi.org/10.1016/j.aca.2019.10.048

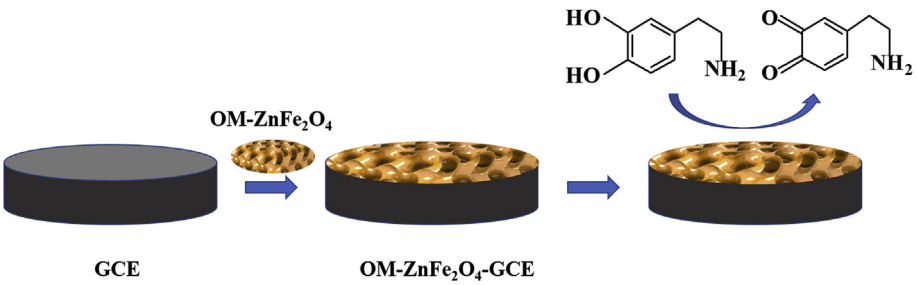

Scheme 1. Illustration for the reaction process of OM-$ZnFe_2O_4$ modified GCE to dopamine.

clearly seen the channels connected to each other through smaller pores and the slit-like pores which are well distributed in the KIT-6. After immersion, calcination and leaching, the OM-$ZnFe_2O_4$ whose ordered mesoporous structure is well preserved can be obtained (Fig. 1(a)-(d)). The typical HRTEM image (Fig. 1(e)) of OM-$ZnFe_2O_4$-40 shows clearly resolved lattice fringes with an interplanar spacing of 0.254 nm, which matches well with the interplanar spacing of (311) plane of $ZnFe_2O_4$ phase [24,25]. The corresponding selected area electron diffraction (SAED) pattern (Fig. 1(f)) reveals a well-defined polycrystalline structure of the as-prepared OM-$ZnFe_2O_4$-40 [26].

The crystal structure of as-prepared OM-$ZnFe_2O_4$ was also examined by XRD (Fig. 2(a)). The diffraction peaks located at 29.96°, 35.74°, 56.62° and 62.77° are well correlated with the (220), (311), (400), (511) and (440) lattice planes of the spinel phase $ZnFe_2O_4$ (JCPDS no. 89—1009). No other phases or impurities are observed, suggesting that the spinel structure of $ZnFe_2O_4$ have been successfully prepared from different hard templates. The texture parameters of mesoporous $ZnFe_2O_4$ were further investigated by nitrogen physisorption and the nitrogen adsorption-desorption isotherms of mesoporous $ZnFe_2O_4$ are given in Fig. 2(b). All isotherms exhibit typical type IV features with H3 hysteresis loops in the relative pressure range of 0.6—1.0 P/P_0 according to the IUPAC classification, signifying the uniform mesoporous structure [27]. The calculated Brunauer-Emmett-Teller (BET) surface area and pore volume are summarized in Table 1. Obviously, the lower the aging temperature of the template, the larger the surface area and pore volume of $ZnFe_2O_4$. It is expected that the higher surface area and larger pore volume of the mesostructure can significantly enhance the catalytic activity of DA detection.

In order to confirm the existence and valence states of Zn, Fe and O in OM-$ZnFe_2O_4$-40, XPS measurements were further conducted. As shown in Fig. 3(a), the full spectrum reveals the co-exist of Zn, Fe and O, and the signal of C may result from the air contamination. More specifically, the peaks around 1022.5 and 1045.5 eV are related to Zn $2p_{3/2}$ and $2p_{1/2}$, which can be attributed to the Zn^{2+} (Fig. 3(b)) [28]. In addition, the binding energies of Fe $2p_{3/2}$ and Fe $2p_{1/2}$ are located at 714.0 and 727.6 eV, respectively (Fig. 3(c)). The results are consistent with the Zn 2p and Fe 2p binding energy for $ZnFe_2O_4$.

3.2. Electrochemical biosensor for detection of DA

Cyclic Voltammetry (CV) was tested to determine the electrochemical properties of bare GCE, OM-$ZnFe_2O_4$-40-GCE, OM-$ZnFe_2O_4$-70-GCE and OM-$ZnFe_2O_4$-100-GCE in PBS electrolyte (pH = 7.0) under a three-electrode system. As shown in Fig. 4(a), each CV curve has a pair of redox peaks with the peak separation

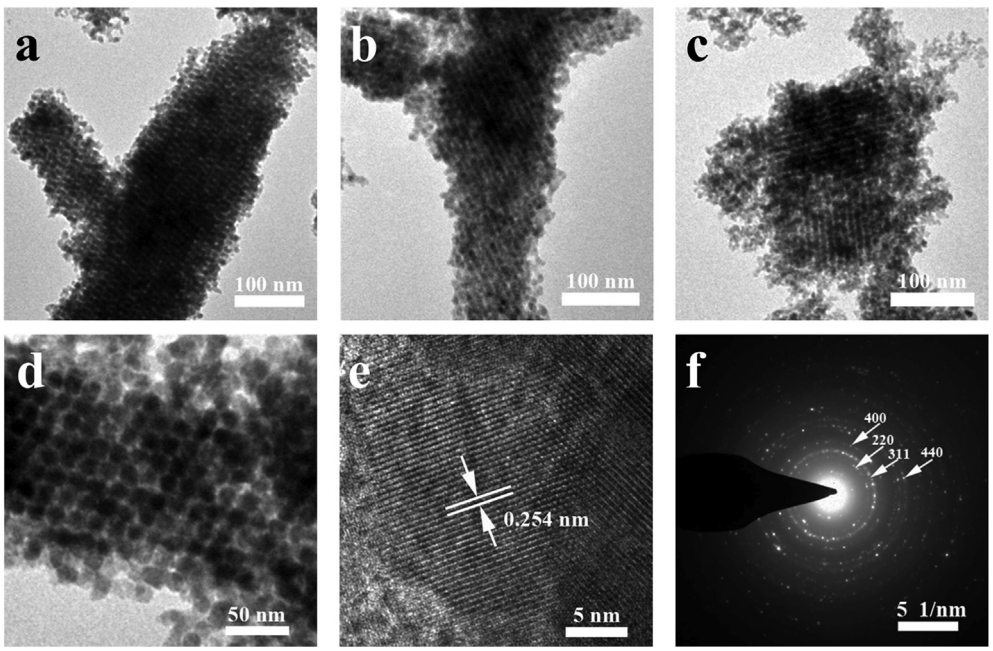

Fig. 1. TEM images of (a, d) OM-$ZnFe_2O_4$-40 with different magnification, (b) OM-$ZnFe_2O_4$-70 and (c) OM-$ZnFe_2O_4$-100. (e) HRTEM image and (f) the corresponding SAED pattern of OM-$ZnFe_2O_4$-40.

Please cite this article as: Y. Huang et al., A highly sensitive sensor based on ordered mesoporous $ZnFe_2O_4$ for electrochemical detection of dopamine, Analytica Chimica Acta, https://doi.org/10.1016/j.aca.2019.10.048

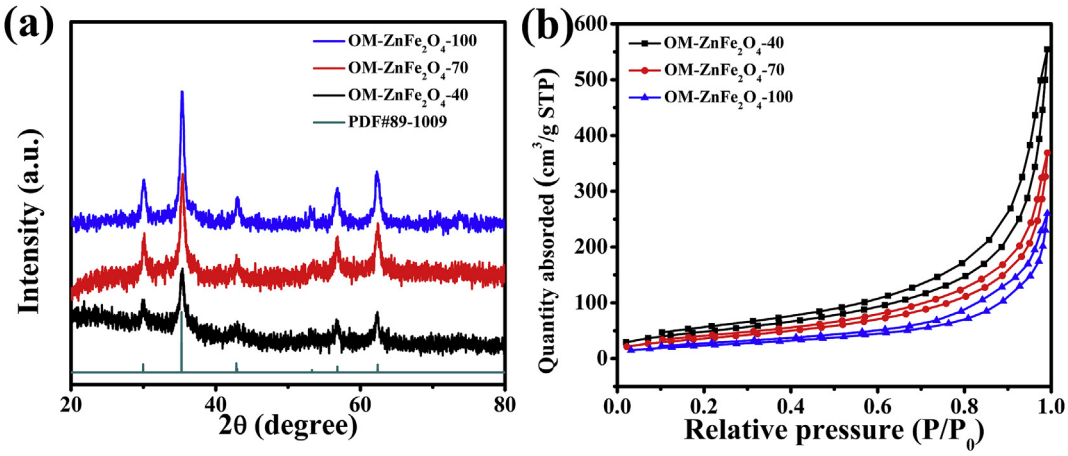

Fig. 2. (a) XRD patterns and (b) N_2 adsorption-desorption isotherms of different OM-$ZnFe_2O_4$.

Table 1
N_2 adsorption desorption isotherm data of as-prepared materials.

Samples	Surface area ($m^2\ g^{-1}$)	Pore volume ($cm^3\ g^{-1}$)
OM-$ZnFe_2O_4$-40	180	0.64
OM-$ZnFe_2O_4$-70	135	0.42
OM-$ZnFe_2O_4$-100	88	0.28

ΔEp at 0. 108 V (on the GCE), 0.046 V (on the OM-$ZnFe_2O_4$-40-GCE), 0.067 V (on the OM-$ZnFe_2O_4$-70-GCE) and 0.095 V (on the OM-$ZnFe_2O_4$-100-GCE), respectively. In contrast, OM-$ZnFe_2O_4$-40-GCE exhibits the much smaller peak separation and higher redox current than those of bare GCE and other OM-$ZnFe_2O_4$-GCE, indicating that the DA redox reversibility of OM-$ZnFe_2O_4$-40-GCE surface is significantly improved, which is because the optimized mesoporous structure not only effectively prevents the aggregation of nanomaterials, but also promotes the exposure of more accessible active sites. As can be seen from Fig. 4(b), the anode and cathode currents increase gradually as the scan rate increases from 10 to 80 mV s^{-1} and the cathodic peak currents increases linearly with the square root of scan rate, where the square of regression coefficient (R^2) is 0.994 (*Inset* of Fig. 4 (b)), indicating the diffusion-controlled electrode process, which is an ideal case for quantitative analysis. The influence effect of pH on the detection of DA by OM-$ZnFe_2O_4$-40-GCE was further investigated via the CV tests in different PBS solution (pH = 3, 5, 7, 9) containing 0.1 mM DA at a scan rate of 100 mV s^{-1} (Fig. 4(c)). With the increase of pH value, the oxidation peak potential shifts negatively, indicating that protons participated in the electrode reaction as the pH increases from 3 to 9. The calculated slope value of −55 mV pH^{-1} is close to the reported theoretical slope value (−59 mV pH^{-1}), which confirms that the electrochemical redox process of DA is a two electrons and two protons process (Fig. 4(d)) [29].

Differential pulse voltammetry (DPV), which has the advantages of improving sensitivity and better analytical applications characteristics, was applied to detect various DA concentration in PBS solution (Fig. 5). The well-defined anode current responses of different OM-$ZnFe_2O_4$-GCE can be observed in the presence of DA (Fig. 5(a)–(c)). The oxidation peak current increases with the DA concentration in the range from 0 to 13 μM for each of the three electrodes. The DPV detection sensitivity can be derived from the linear regression equation (Fig. 5(d)), and the OM-$ZnFe_2O_4$-40-GCE exhibits a much higher sensitivity of 1.455 μA μM^{-1} (I_{pa} (μA) = 1.455 C (μM) - 0.342 (R^2 = 0.996)) compared to either the OM-$ZnFe_2O_4$-70-GCE (I_{pa} (μA) = 1.195 C (μM) − 0.060 (R^2 = 0.998)) or the OM-$ZnFe_2O_4$-100-GCE (I_{pa} (μA) = 1.065 C (μM) + 0.051 (R^2 = 0.990)). All the modified electrodes exhibit a leaner relationship with DA concentration.

The amperometric current-time responses of OM-$ZnFe_2O_4$-40-GCE, OM-$ZnFe_2O_4$-70-GCE and OM-$ZnFe_2O_4$-100-GCE for the addition of different concentrations of DA in 0.1 M PBS at an applied potential of 0.23 V (*vs.* Ag/AgCl) are given in Fig. 6(a). A well-defined amoperometric response was observed upon each addition of DA solution, and the response time is within 5 s. When the addition concentration of DA is 2 nM, the obvious signal also can be produced, which can be clearly seen in Fig. 6(b). The calibration plot

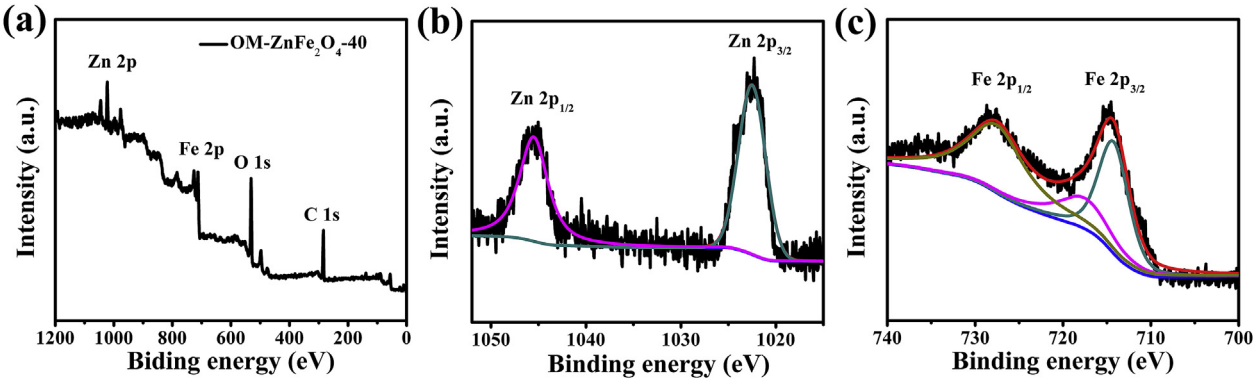

Fig. 3. XPS spectra of (a) full spectrum, (b) Zn 2p and (c) Fe 2p regions of OM-$ZnFe_2O_4$-40.

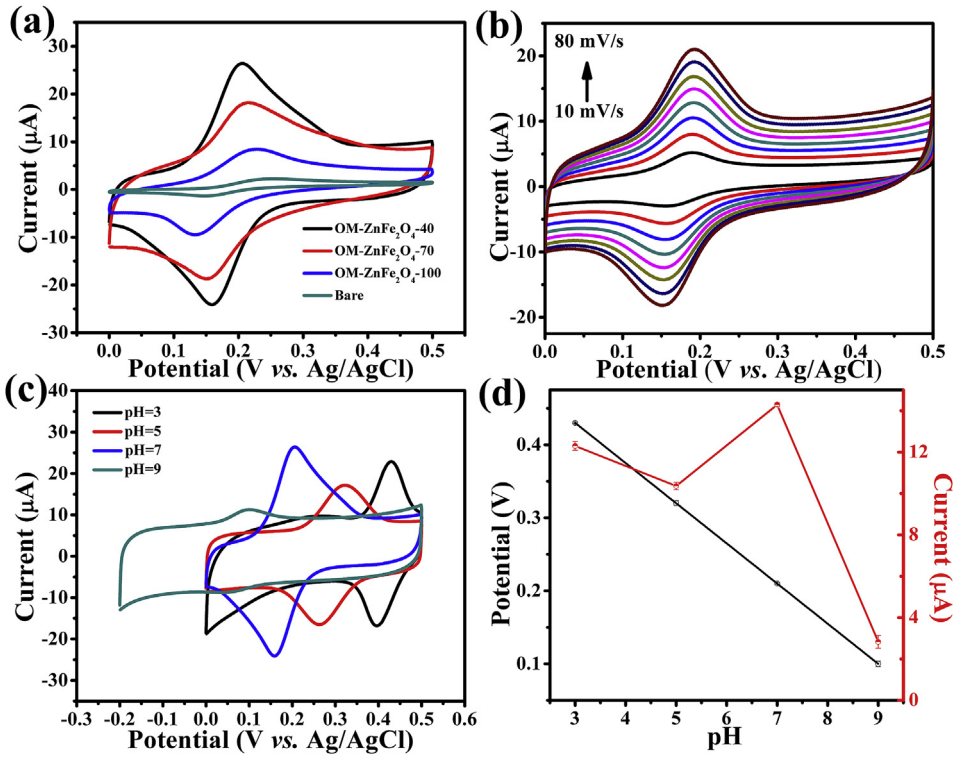

Fig. 4. (a) CVs of bare GCE, OM-$ZnFe_2O_4$-40-GCE, OM-$ZnFe_2O_4$-70-GCE and OM-$ZnFe_2O_4$-100-GCE, respectively, at a scan rate of 100 mV s^{-1} in PBS solution (pH 7.0) containing 0.1 mM DA. (b) CV curves of OM-$ZnFe_2O_4$-40-GCE at various scan rates from 10 to 80 mV s^{-1} (*Inset*: Plot of peak current *vs*. square root of scan rates.). (c) CV curves of OM-$ZnFe_2O_4$-40-GCE in PBS with different pH (pH = 3, 5, 7, 9) containing 0.1 mM DA, scan rate: 100 mV s^{-1}. (d) The plots of E_{pa} (black) and I_{pa}(red) with different pH values. (For interpretation of the references to color in this figure legend, the reader is referred to the Web version of this article.)

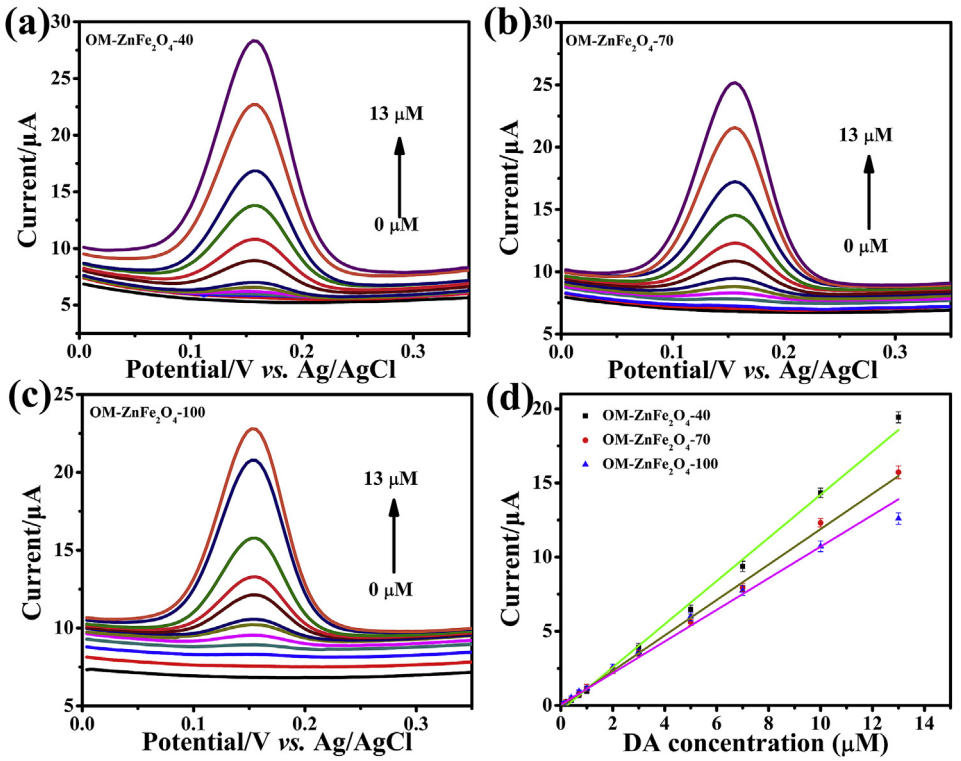

Fig. 5. DPV curves of 0 μM−13 μM DA at (a) OM-$ZnFe_2O_4$-40-GCE, (b) OM-$ZnFe_2O_4$-70-GCE and (c) OM-$ZnFe_2O_4$-100-GCE, respectively, in 0.1 M PBS solution (pH 7.0). Pulse width: 10 ms, amplitude: 50 mV. (d) Plots of the oxidation peak currents *vs*. DA concentration for the OM-$ZnFe_2O_4$-40-GCE, OM-$ZnFe_2O_4$-70-GCE and OM-$ZnFe_2O_4$-100-GCE.

Please cite this article as: Y. Huang et al., A highly sensitive sensor based on ordered mesoporous $ZnFe_2O_4$ for electrochemical detection of dopamine, Analytica Chimica Acta, https://doi.org/10.1016/j.aca.2019.10.048

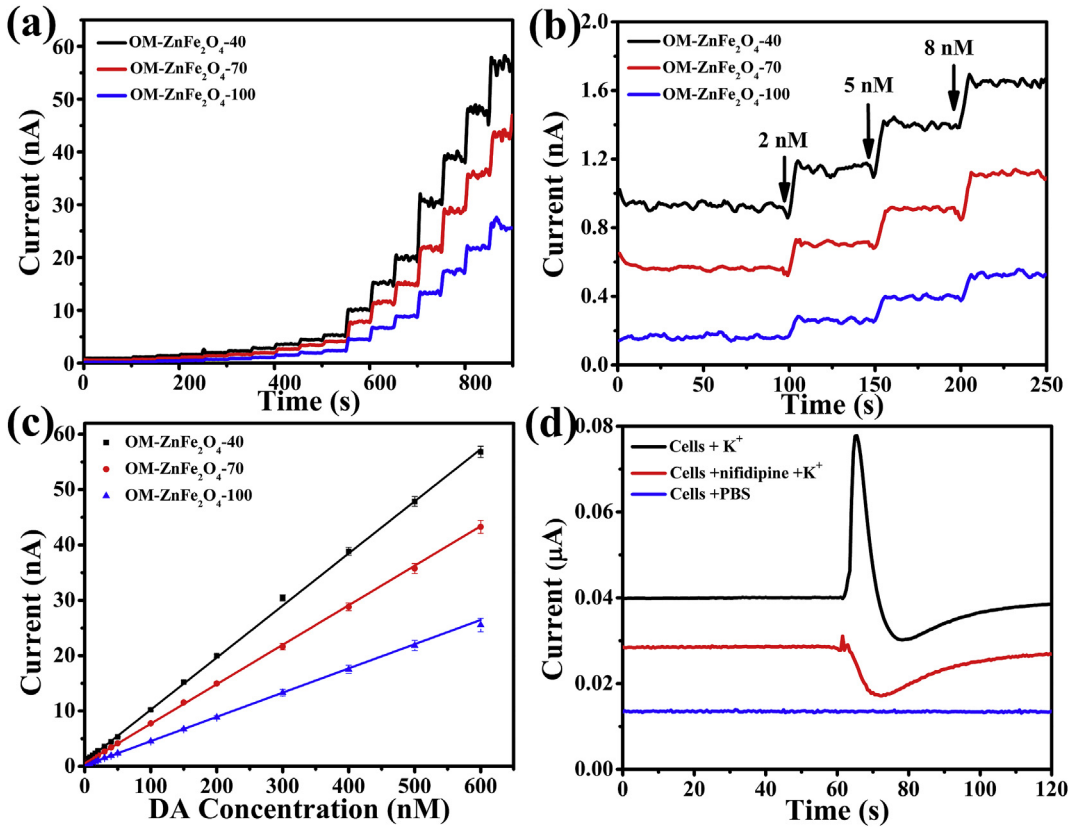

Fig. 6. (a) Amperometric current-time responses of the various OM-$ZnFe_2O_4$-GCE on the successive addition of DA in PBS (pH 7.0) at an applied potential of 0.23 V (*vs.* Ag/AgCl). (b) The partial enlargement of (a) from 0s to 250s. (c) The dependence of the current response of the OM-$ZnFe_2O_4$-GCE on the DA concentration. (d) A characteristic current-time response recorded for dopamine released from PC12 cells at OM-$ZnFe_2O_4$-40 upon stimulating with a 100 mM KCl solution (black) at a potential of 0.23 V *vs.* Ag/AgCl. After being treated with nifedipine (50 μM) for 30 min, the cells were stimulated with the same concentrations of K^+ solutions (red). Addition of PBS instead of high K^+ buffer at OM-$ZnFe_2O_4$-40 in the presence of PC12 cells (blue). The arrow indicates the time of addition of high K^+ buffer. (For interpretation of the references to color in this figure legend, the reader is referred to the Web version of this article.)

(Fig. 6(c)) was linearly proportional to the dopamine amount over the range of 2 nM–600 nM. The linear regression equation was expressed as: I_{pa} (nA) = 0.094 C (nM) + 0.813 ($R^2 = 0.998$)) (OM-$ZnFe_2O_4$-40-GCE), I_{pa} (nA) = 0.071 C (nM) + 0.56 ($R^2 = 0.999$)) (OM-$ZnFe_2O_4$-70-GCE) and I_{pa} (nA) = 0.044 C (nM) + 0.171 ($R^2 = 0.999$)) (OM-$ZnFe_2O_4$-100-GCE). Moreover, based on a signal-to-noise ratio (S/N) of 3, the detection limit of 0.4 nM can be obtained from OM-$ZnFe_2O_4$-40-GCE, which is lower than that of OM-$ZnFe_2O_4$-70-GCE (0.5 nM) and OM-$ZnFe_2O_4$-100-GCE (1 nM). The excellent properties of OM-$ZnFe_2O_4$ for DA detection can be attribute to the ability of mesoporous structures to rapidly adsorb and activate DA molecules, as well as their high surface area and large pore volume. Table 2 summarizes the analytical performance of the proposed sensor and the other reported sensors for DA detection. Furthermore, 10-fold concentration of NaCl, uric acid and ascorbic acid were injected as interferences, no DPV response was observed (Fig. S2), indicating that the OM-$ZnFe_2O_4$-40-GCE possess the excellent selectivity towards DA. In addition, CV was employed to evaluate the reproducibility of OM-$ZnFe_2O_4$-40-GCE and the reproducibility of 5 different OM-$ZnFe_2O_4$-40-GCE is found with an RSD (relative standard deviation) of 3.1% for detection of 0.1 mM DA. There are no obvious changes after comparing the 7 days stability tests. Finally, we investigated the potential application of OM-$ZnFe_2O_4$-40-GCE electrode in real sample analysis by analyzing the DA released from PC12 cells in living states. Amperometric current-time trace was recorded during potassium-induced DA exocytosis from a population of PC12 cells. As shown in Fig. 6(d) (black), an obvious current response originated from DA oxidation was observed after adding 100 mM KCl, confirming that the traced amounts of DA released from a living cell can be detected rapidly by the OM-$ZnFe_2O_4$-40-GCE. The number of detected DA is calculated to be 6.65×10^{11} according the equation: $N = Q/nQ_e$. The

Table 2
Comparison of OM-$ZnFe_2O_4$ DA sensors with other electrochemical sensors for detection of DA.

Electrode materials	Methods	Dynamic ranges (μM)	Detection limits (nM)	Refs
TiC/CNFs	DPV	0.05–45	20	[30]
dumbbell-like FePt–Fe_3O_4	Amperometry	0.005-0.11	1	[31]
AuNPs@MoS_2-NSs	DPV	5.0–200	1000	[32]
NiO–CuO/GR/GCE	DPV	0.3–40	100	[33]
$NCCNPs_{800}$/GCE	DPV	2–69.5	340	[34]
Flower shaped ZnO	DPV	0.1–16	40	[35]
OM-$ZnFe_2O_4$-40	Amperometry	0.002-0.6	0.4	This work

Please cite this article as: Y. Huang et al., A highly sensitive sensor based on ordered mesoporous $ZnFe_2O_4$ for electrochemical detection of dopamine, Analytica Chimica Acta, https://doi.org/10.1016/j.aca.2019.10.048

stimulation of K^+ make PC12 cells exocytosis and release DA, which causes depolarization of the cell membrane and induces an influx of Ca^{2+} through opening of voltage-sensitive Ca^{2+} channels [36]. In order to validate the observed signal was not caused by the response of the proposed sensor to K^+ stimulation, only PBS solution contain the PC12 cells solution sample that was no K^+ stimulation was prepared to perform control experiments (Fig. 6(d), blue), no current response was observed in the control experiments. It is reported that nifidipine have the ability to inhibit the K^+ stimulation. Therefore, we treated the PC12 cells with 50 μM nifidipine for 30 min, and then added 100 mM KCl for stimulation. A weak current spike was observed (Fig. 6(d), red), which indicates that the current response is not caused by K^+ or only the cells. These results suggest that OM-$ZnFe_2O_4$-40-GCE has the potential to be an efficient sensor for detecting DA in biological solution.

4. Conclusions

A highly sensitive DA sensor has been synthesized successfully by a facial hard template nanocasting method. The OM-$ZnFe_2O_4$ sensor with high surface area and large pore volume for DA detection was investigated systematically. OM-$ZnFe_2O_4$ modified GCE shows highly sensitive and selective for detecting DA at a low concentration owe to the mesoporous structure which can enable fast adsorption, activation of DA molecules and efficient electron transport. OM-$ZnFe_2O_4$-40-GCE displays the lowest detection limit of 0.4 nM (S/N = 3) with a large linear range between 2 nM and 600 nM, which is good enough for analyzing DA levels in clinical applications. The fabricated sensor also shows excellent performance for real-time detection of DA released from PC12 cells. This work gives a new route for designing highly sensitive and selective electrochemical sensors for practical applications based on ordered mesoporous nanomaterials.

Declaration of competing interest

The authors declare that they have no known competing financial interests or personal relationships that could have appeared to influence the work reported in this paper.

Acknowledgements

This work was supported by the National Natural Science Foundation of China under Grant (No. 21305025, 51571072, 51871078 and 81771508), Heilongjiang Science Foundation (No. E2018028) and Key Laboratory of Functional Materials Physics and Chemistry of the Ministry of Education (Nos. 2017001 and 2017002).

Appendix A. Supplementary data

Supplementary data to this article can be found online at https://doi.org/10.1016/j.aca.2019.10.048.

References

[1] J.J. Jiang, X.Z. Du, Sensitive electrochemical sensors for simultaneous determination of ascorbic acid, dopamine, and uric acid based on Au@Pd-reduced graphene oxide nanocomposites, Nanoscale 6 (2014) 11303–11309.
[2] S. Sansuk, E. Bitziou, M.B. Joseph, J.A. Covington, M.G. Boutelle, et al., Ultrasensitive detection of dopamine using a carbon nanotube network microfluidic flow electrode, Anal. Chem. 85 (2013) 163–169.
[3] M.D. Rubianes, A.S. Arribas, E. Bermejo, M. Chicharro, A. Zapardiel, et al., Carbon nanotubes paste electrodes modified with a melanic polymer: analytical applications for the sensitive and selective quantification of dopamine, Sens. Actuators B Chem. 144 (2010) 274–279.
[4] S.Y. Zhu, H.J. Li, W.X. Niu, G.B. Xu, Simultaneous electrochemical determination of uric acid, dopamine, and ascorbic acid at single-walled carbon nanohorn modified glassy carbon electrode, Biosens. Bioelectron. 25 (2009) 940–943.
[5] H.H. Wang, X.J. Chen, W.T. Li, W.H. Zhou, X.C. Guo, et al., ZnO nanotubes supported molecularly imprinted polymers arrays as sensing materials for electrochemical detection of dopamine, Talanta 176 (2018) 573–581.
[6] J. Shen, C.M. Sun, X. Wu, Silver nanoprisms-based Tb(III) fluorescence sensor for highly selective detection of dopamine, Talanta 165 (2017) 369–376.
[7] Y.M. Len, K. Xie, L.Q. Ye, G.Q. Li, Z.W. Lu, et al., Gold-nanoparticle-based colorimetric array for detection of dopamine in urine and serum, Talanta 139 (2015) 89–95.
[8] J. Oh, J.S. Lee, J. Jun, S.G. Kim, J. Jang, Ultrasensitive and selective organic FET-type nonenzymatic dopamine sensor based on platinum nanoparticles-decorated reduced graphene oxide, ACS Appl. Mater. Interfaces (9) (2017) 39526–39533.
[9] M.S. Hsu, Y.L. Chen, C.Y. Lee, H.T. Chiu, Gold nanostructures on flexible substrates as electrochemical dopamine sensors, ACS Appl. Mater. Interfaces 4 (2012) 5570–5575.
[10] M.H. Yang, J.M. Jeong, K.G. Lee, D.H. Kim, S.J. Lee, et al., Hierarchical porous microspheres of the Co_3O_4@graphene with enhanced electrocatalytic performance for electrochemical biosensors, Biosens. Bioelectron. 89 (2017) 612–619.
[11] G. Gao, Z.K. Zhang, K. Wang, Q. Yuan, X. Wang, One-pot synthesis of dendritic Pt_3Ni nanoalloys as nonenzymatic electrochemical biosensors with high sensitivity and selectivity for dopamine detection, Nanoscale 9 (2017) 10998–11003.
[12] Q.J. Lu, X.G. Chen, D. Liu, C.Y. Wu, M.L. Liu, et al., Synergistic electron transfer effect-based signal amplification strategy for the ultrasensitive detection of dopamine, Talanta 182 (2018) 428–432.
[13] N. Yusoff, A. Pandikumar, R. Ramaraj, H.N. Lim, N.M. Huang, Gold nanoparticle based optical and electrochemical sensing of dopamine, Microchim. Acta 182 (2015) 2091–2114.
[14] H.Y. Xu, M.W. Shao, T. Chen, S.J. Zhuo, C.Y. Wen, et al., Magnetism-assisted assembled porous Fe_3O_4 nanoparticles and their electrochemistry for dopamine sensing, Microporous Mesoporous Mater. 153 (2012) 35–40.
[15] A.F. Shojaei, K. Tabatabaeian, S. Shakeri, F. Karimi, A novel 5-fluorouracile anticancer drug sensor based on $ZnFe_2O_4$ magnetic nanoparticles ionic liquids carbon paste electrode, Sens. Actuators B Chem. 230 (2016) 607–614.
[16] N. Tavakkoli, N. Soltani, F. Shahdost-fard, M. Ramezani, H. Salavati, et al., Simultaneous voltammetric sensing of acetaminophen, epinephrine and melatonin using a carbon paste electrode modified with zinc ferrite nanoparticles, Microchim. Acta 185 (2018) 479–480.
[17] M.G. Zhao, S.S. Fan, J.J. Liang, Y. Liu, Y.C. Li, et al., Synthesis of mesoporous grooved $ZnFe_2O_4$ nanobelts as peroxidase mimetics for improved enzymatic biosensor, Ceram. Int. 41 (2015) 10400–10405.
[18] K.L. Parent, D.F. Hill, L.M. Crown, J.P. Wiegand, K.F. Gies, et al., Platform to enable combined measurement of dopamine and neural activity, Anal. Chem. 89 (2017) 2790–2799.
[19] S. Demuru, L. Nela, N. Marchack, S.J. Holmes, D.B. Farmer, et al., Scalable nanostructured carbon electrode arrays for enhanced dopamine detection, ACS Sens. 3 (2018) 799–805.
[20] J. Manna, S. Akbayrak, S. Özkar, Palladium(0) nanoparticles supported on polydopamine coated $CoFe_2O_4$ as highly active, magnetically isolable and reusable catalyst for hydrogen generation from the hydrolysis of ammonia borane, Appl. Catal. B Environ. 208 (2017) 104–115.
[21] B. Cai, M.G. Zhao, Y. Ma, Z.Z. Ye, J.Y. Huang, Bioinspired formation of 3D hierarchical $CoFe_2O_4$ porous microspheres for magnetic-controlled drug release, ACS Appl. Mater. Interfaces 7 (2015) 1327–1333.
[22] W.N. Yan, X.C. Cao, J.H. Tian, C. Jin, K. Ke, et al., Nitrogen/sulfur dual-doped 3D reduced graphene oxide networks-supported $CoFe_2O_4$ with enhanced electrocatalytic activities for oxygen reduction and evolution reactions, Carbon 99 (2016) 195–202.
[23] X.H. Deng, K. Chen, H. Tüysüz, Protocol for the nanocasting method: preparation of ordered mesoporous metal oxides, Chem. Mater. 29 (2017) 40–52.
[24] X.M. Gao, Y. Sun, C.L. Zhu, C.Y. Li, Q.Y. Ouyang, et al., Highly sensitive and selective H_2S sensor based on porous $ZnFe_2O_4$ nanosheets, Sens. Actuators B Chem. 246 (2017) 662–672.
[25] L. Li, J.F. Tan, M.H. Dun, X.T. Huang, Porous $ZnFe_2O_4$ nanorods with networked nanostructure for highly sensor response and fast response acetone gas sensor, Sens. Actuators B Chem. 248 (2017) 85–91.
[26] H.J. Zhang, F.N. Meng, L.Z. Liu, Y.J. Chen, P.J. Wang, Highly sensitive H_2S sensor based on solvothermally prepared spinel $ZnFe_2O_4$ nanoparticles, J. Alloy. Comp. 764 (2018) 147–154.
[27] C.L. Xiao, X.Y. Zhang, T. Mendes, G.P. Knowles, A. Chaffee, Highly ordered hierarchical mesoporous $MnCo_2O_4$ with cubic $I\alpha3d$ symmetry for electrochemical energy storage, J. Phys. Chem. C 120 (2016) 23976–23983.
[28] Z. Xing, Z.C. Ju, J. Yang, H.Y. Xu, Y.T. Qian, One-Step hydrothermal synthesis of $ZnFe_2O_4$ nano-octahedrons as a high capacity anode material for Li-ion batteries, Nano. Res. 5 (2012) 477–485.
[29] B. Thirumalraj, S. Palanisamy, S.M. Chen, B.S. Lou, Preparation of highly stable fullerene C60 decorated graphene oxide nanocomposite and its sensitive electrochemical detection of dopamine in rat brain and pharmaceutical samples, J. Colloid Interface Sci. 462 (2016) 375–381.
[30] Q.H. Guo, T.T. Wu, L.J. Liu, H.Q. Hou, S.L. Chen, et al., Flexible and conductive titanium carbide-carbon nanofibers for the simultaneous determination of

ascorbic acid, dopamine and uric acid, J. Mater. Chem. B 6 (2018) 4610–4617.
[31] W.W. Yang, Y.S. Yu, Y. Tang, K.Y. Li, Z. Zhao, et al., Enhancing electrochemical detection of dopamine via dumbbell-like FePt-Fe_3O_4 nanoparticles, Nanoscale 9 (2017) 1022–1027.
[32] H.L. Zou, B.L. Li, H.Q. Luo, N.B. Li, 0D-2D heterostructures of Au nanoparticles and layered MoS_2 for simultaneous detections of dopamine, ascorbic acid, uric acid, and nitrite, Sens. Actuators B Chem. 253 (2017) 352–360.
[33] B.D. Liu, X.Q. Ouyang, Y.P. Ding, L.Q. Luo, D. Xu, et al., Electrochemical preparation of nickel and copper oxides-decorated graphene composite for simultaneous determination of dopamine, acetaminophen and tryptophan, Talanta 146 (2016) 114–121.
[34] H.L. Guo, M. Wang, L. Zhao, N. Youliwasi, C.G. Liu, The effect of Co and N of porous carbon-based materials fabricated via sacrificial templates MOFs on improving DA and UA electrochemical detection, Micropor. Mosopor. Mat. 263 (2018) 21–27.
[35] D. Balram, K.Y. Lian, N. Sebastian, A novel electrochemical sensor based on flower shaped zinc oxide nanoparticles for the efficient detection of dopamine, Int. J. Electrochem. Sci. 13 (2018) 1542–1555.
[36] T.A. Mir, M.H. Akhtar, N.G. Gurudatt, J.I. Kim, C.S. Choi, et al., An amperometric nanobiosensor for the selective detection of K^+-induced dopamine released from living cell, Biosens. Bioelectron. 68 (2015) 421–428.

Please cite this article as: Y. Huang et al., A highly sensitive sensor based on ordered mesoporous $ZnFe_2O_4$ for electrochemical detection of dopamine, Analytica Chimica Acta, https://doi.org/10.1016/j.aca.2019.10.048